THE ASTROPHYSICAL JOURNAL, 576:574–586, 2002 September 1
© 2002. The American Astronomical Society. All rights reserved. Printed in U.S.A.

THE TRANSPORT OF CHARGED PARTICLES IN A FLOWING MEDIUM

J. Y. LU[1]
Department of Physics, University of Alberta, Edmonton, AB T6G 2J1, Canada; jlu@space.ualberta.ca

G. P. ZANK
Institute of Geophysics and Planetary Physics, University of California, Riverside, CA 92521; zank@ucrac1.ucr.edu

AND

R. RANKIN AND R. MARCHAND
Department of Physics, University of Alberta, Edmonton, AB T6G 2J1, Canada; rankin@space.ualberta.ca, marchand@phys.ualberta.ca
Received 2002 February 18; accepted 2002 May 10

ABSTRACT

The propagating source method for solving the time-dependent Boltzmann equation describing particle propagation in a magnetically turbulent medium is extended to a more realistic case that includes focusing and adiabatic deceleration. The solutions correspond to beam propagation in the solar wind. Pitch-angle scattering away from 90° is described by standard quasi-linear theory (QLT), while scattering through 90° is approximated by a BGK operator representing a slow mirroring process. The detailed numerical technique for solving the Fokker-Planck equation for two particular spectra is presented. Comparisons are made between our modified QLT (MQLT) model and a BGK model, between highly anisotropic scattering and moderately anisotropic scattering, and between fast particles and slow particles. It is shown that: (1) for moderately anisotropic pitch-angle scattering, the initial ring-beam distribution finally evolves into a broad Gaussian distribution and the QLT isotropic and MQLT anisotropic models could be rather well approximated by the simple relaxation time operator. (2) For highly anisotropic pitch-angle scattering, a moving pulse with a spatially extended flat tail is formed, and there exist some differences between the MQLT and BGK models. Specifically, at a particular pitch angle, the spatial distribution from MQLT model occupies a much wider region than that in the BGK model. (3) In the highly anisotropic scattering medium, more particles are cooled by adiabatic deceleration, some particles move a little faster, and the spatial distribution at a specific pitch angle is much more dispersed than that in the case of moderately anisotropic scattering. (4) Compared with the BGK model, the anisotropy persists for a little longer and some particles move a little slower; consequently, intensity profiles have a greater amplitude at later times in the MQLT model. (5) Finally, fast and slow particles have similar distribution characteristics, except that convection is much more important for slow particles.

Subject headings: acceleration of particles — cosmic rays — methods: numerical — plasmas — solar wind

On-line material: color figures

1. INTRODUCTION

Pitch-angle scattering in random magnetic fields is one of the basic mechanisms that control the propagation of charged particles in space or astrophysical environments. Thus, particle populations such as Galactic and anomalous cosmic rays, energetic solar particles, and interstellar and cometary pickup ions have distributions that are shaped by pitch-angle scattering. Since magnetic fluctuations are present in the solar wind (and undoubtedly in the interstellar medium as well) on all scales and amplitudes, particle transport is likely to be a combination of small-angle and large-angle scattering. We have written a series of papers to introduce a new approach, the propagating source method, to solve the time-dependent transport equation for charged particles: Zank et al. (2000, hereafter Paper I) solved the BGK Boltzmann equation under the assumptions of isotropic pitch-angle scattering and large particle energies. Lu, Zank, & Webb (2001, hereafter Paper II) extended Paper I and developed a numerical solution for fast and slow particles experiencing anisotropic pitch-angle scattering. The scattering was modeled by a two-timescale BGK operator, and the model was subsequently applied to investigate the propagation of interstellar pickup ions (Lu & Zank 2001). Recently, the propagating source method was extended to the quasi-linear scattering operator (Zank, Lu, & Dröge 2002, hereafter Paper III), but was limited by the neglect of focusing and adiabatic deceleration. Here we extend the propagating source method to a more realistic Boltzmann equation that includes focusing and adiabatic deceleration, and compare large-angle and small-angle scattering models.

[1] Also at Center for Space Science and Applied Research, Chinese Academy of Sciences, Beijing, China.

The transport of charged particles along a magnetic field is governed by the Fokker-Planck equation. By assuming that the charged particle distribution function $f(\boldsymbol{x}, t, \boldsymbol{v})$ is nearly gyrotropic, the gyrophase-averaged Boltzmann equation in a stationary frame can be expressed as (Skilling 1971; Kulsrud 1983; Isenberg 1997)

$$\frac{\partial f}{\partial t} + (U_i + v\mu b_i)\frac{\partial f}{\partial x_i} + \left[\frac{1-3\mu^2}{2} b_i b_j \frac{\partial U_i}{\partial x_j} - \frac{1-\mu^2}{2}\frac{\partial U_i}{\partial x_i} - \frac{\mu b_i}{v}\left(\frac{\partial U_i}{\partial t} + U_j \frac{\partial U_i}{\partial x_j}\right)\right] v \frac{\partial f}{\partial v}$$
$$+ \frac{1-\mu^2}{2}\left[v\frac{\partial b_i}{\partial x_i} + \mu\frac{\partial U_i}{\partial x_i} - 3\mu b_i b_j \frac{\partial U_i}{\partial x_j} - \frac{2b_i}{v}\left(\frac{\partial U_i}{\partial t} + U_j\frac{\partial U_i}{\partial x_j}\right)\right]\frac{\partial f}{\partial \mu} = \left(\frac{\delta f}{\delta t}\right)_c + S - L\,. \quad (1)$$

In equation (1), the distribution function $f(\boldsymbol{x}, t, \boldsymbol{v}) = f(\boldsymbol{x}, t, \mu, v)$, where the pitch angle $\mu \equiv \boldsymbol{v} \cdot \boldsymbol{b}/\boldsymbol{v} = \cos\theta$, $\boldsymbol{b} = \boldsymbol{B}/|\boldsymbol{B}|$ is the unit vector aligned with the large-scale magnetic field $\boldsymbol{B}$, v denotes the particle speed, and v and μ refer to the plasma reference frame. Here $\boldsymbol{U}$ is the large-scale bulk flow velocity. The variables x and t denote the particle position and time, respectively, and $(\delta f/\delta t)_c$ is the pitch-angle scattering operator. The terms S and L are source and loss terms, respectively. We do not consider energy diffusion, perpendicular diffusion, drift, or sources and losses, but restrict ourselves to a constant flow speed U and radial magnetic field. Then, equation (1) reduces to

$$\frac{\partial f}{\partial t} + (U + \mu v)\frac{\partial f}{\partial r} - \frac{1-\mu^2}{r} u v \frac{\partial f}{\partial v} + \frac{1-\mu^2}{r}(v + \mu U)\frac{\partial f}{\partial \mu} = \left(\frac{\delta f}{\delta t}\right)_c . \quad (2)$$

The pitch-angle scattering operator $(\delta f/\delta t)_c$ is given usually by weak turbulence quasi-linear theory (QLT),

$$\left(\frac{\delta f}{\delta t}\right)_c = \frac{\partial}{\partial \mu}\left(D_{\mu\mu}\frac{\partial f}{\partial \mu}\right) , \quad (3)$$

with the coefficient of pitch-angle scattering given by (Jokipii 1966; Hasselmann & Wibberenz 1968)

$$D_{\mu\mu} = \frac{|\mu|^{q-1}(1-\mu^2)}{\tau} , \quad (4)$$

where q is the spectral index of magnetic field turbulence, and τ is the effective scattering time [$\tau = 3\tau_s/(2-q) \times (4-q)$; τ_s is the scattering time].

Although QLT has been applied to explain many space or astrophysical problems, it obviously fails at producing scattering through $\mu = 0$, and the 90° problem has not yet been resolved. The BGK collision operator or relaxation-time approximation is sometimes used instead of equation (3) (Fisk & Axford 1969; Gombosi et al. 1993; Kóta 1994; Schwadron 1998; Lu & Zank 2001). In attempting to resolve the 90° problem associated with QLT, several modifications to QLT have been suggested. Among these are mirroring by fluctuations of the magnetic field magnitude (Goldstein, Klimas, & Sandri 1975; Smith 1992), nonlinear extensions of QLT (Goldstein 1976; Jones, Birmingham, & Kaiser 1978; Owens 1974; Völk 1975), resonance broadening (Völk 1973), wave-propagation effects (Schlickeiser 1988, 1989; Schlickeiser, Dung, & Haekel 1991; Dröge & Schlickeiser 1993; Dröge 2000a), dynamical turbulence (Bieber & Matthaeus 1991, 1992; Bieber et al. 1994), and nonresonant pitch-angle scattering (Ragot 1999, 2000). A review of models describing various approaches to particle scattering through 90° is given by Dröge (2000b). By using a simple model, Paper III considered four augmentations to QLT and compared the behavior of different scattering mechanisms through 90°. In this paper we neither discuss those mechanisms nor suggest any new mechanism. Our purpose is to develop a new numerical approach to solving the Fokker-Planck equation.

Recently, Felice & Kulsrud (2001) presented a self-consistent theory that attempts to resolve the problem of scattering through 90° by including a mirror interaction with self-generated waves. In their model, QLT is assumed to hold to down to a value of $\mu = 10^{-4}$. Mirror effects and the quasi-linear wave interactions act over all pitch angles, after which the mirror-linear interaction dominates for $\theta \sim 90°$. As noted, quasi-linear interactions dominate outside of the small region.

In this paper, we use an assumption similar to that of Felice & Kulsrud (2001): the quasi-linear interaction holds within the forward and backward hemisphere, while the mirror-linear interaction is responsible for the scattering through 90°. We introduce two scattering timescales, τ_1 and τ_2, where τ_1 is the quasi-linear pitch-angle scattering time, and τ_2 is mirroring scattering time. In order to distinguish our approach from the standard QLT model, we refer to it here as the MQLT model.

2. ISOTROPIC SMALL-ANGLE SCATTERING MODEL

Consider first the special case of $q = 1$, which corresponds to isotropic scattering with no singularity at 90° in equation (4). If we assume a constant radial flow as the background, and a large-scale magnetic field pointing away from the Sun, the

Boltzmann equation (2) becomes

$$\frac{\partial f}{\partial t} + (U + v\mu)\frac{\partial f}{\partial r} - \frac{1-\mu^2}{r}Uv\frac{\partial f}{\partial v} + \frac{1-\mu^2}{r}(v + \mu U)\frac{\partial f}{\partial \mu} = \frac{\partial}{\partial \mu}\left(\frac{1-\mu^2}{\tau}\frac{\partial f}{\partial \mu}\right) , \tag{5}$$

where τ is the quasi-linear small-angle scattering time. As in Papers I, II, and III, we consider the Cauchy problem of equation (5) with arbitrary initial data given by

$$f(r, t = 0, \mu, v) = F(r, 0, \mu, v) . \tag{6}$$

Note that no restrictions are imposed on the form of the initial data, i.e., they need not be isotropic, and we consider an initial ring-beam distribution

$$F(r, 0, \mu, v) = \frac{N(r)\delta(v - v_0)\delta(\mu - \mu_0)}{2\pi v^2} , \tag{7}$$

where $N(r)$ is the particle number density as a function of position. We shall frequently consider a localized number density $N(r) = H(r - r_1) - H(r - r_2)$ between r_1 and r_2 (where H is the Heaviside step function). Throughout this paper, the subscript "0" denotes the parameter values of particles in a ring-beam distribution.

As discussed in Papers I and II (also see Gombosi et al. 1993) in the context of large-angle scattering, at very early times an initial particle distribution should propagate almost ballistically until such time as scattering begins to modify the distribution. Thus, particle scattering may be viewed as a loss process for the unscattered streaming particles with a decay time given by the scattering time τ. Conversely, no scattered particles exist at early times, and instead the scattered distribution grows from zero as the unscattered streaming distribution decays. Thus, initial data can be prescribed for the unscattered particle distribution, which, as it decays, leads to the formation of a scattered particle distribution. This approach was discussed originally by Zank et al. (1999) and is reminiscent of the multiple scattering solution of the Boltzmann equation presented by Webb et al. (1999). Since we are at liberty to separate the distribution function in any way we choose, provided that we ensure that the appropriate initial and boundary conditions hold, the above comments suggest that we split the distribution function f into an "unscattered" part F and a "scattered" part f^s according to the decomposition

$$f = F + f^s . \tag{8}$$

A similar separation has been used by Gombosi et al. (1991), Zank et al. (1999), Fedorov, Stehlik, & Kudela (1999), Webb, Pantazopoulou, & Zank (2000), and Lu & Zank (2001). Since the unscattered part F experiences no scattering and is therefore not described by a diffusion term in μ, equation (5) can be expressed as

$$\frac{\partial F}{\partial t} + (U + \mu v)\frac{\partial F}{\partial r} - \frac{1-\mu^2}{r}Uv\frac{\partial F}{\partial v} + \frac{1-\mu^2}{r}(v + \mu U)\frac{\partial F}{\partial \mu} = -\frac{F}{\tau} , \tag{9}$$

$$\frac{\partial f^s}{\partial t} + (U + \mu v)\frac{\partial f^s}{\partial r} - \frac{1-\mu^2}{r}Uv\frac{\partial f^s}{\partial v} + \frac{1-\mu^2}{r}(v + \mu U)\frac{\partial f^s}{\partial \mu} = \frac{\partial}{\partial \mu}\left(\frac{1-\mu^2}{\tau}\frac{\partial f^s}{\partial \mu}\right) + \frac{F}{\tau} . \tag{10}$$

Note that F can only lose particles unless an explicit source term is present (such as occurs for pickup ions in the inner and outer heliosphere; Lu & Zank 2001). Evidently, F is a source term for the scattered particle distribution and, unlike the prescribed initial data, is a moving source. As discussed in Paper I, such a distributed source of scattered particles acts to eliminate the possibility of coherent pulses forming for isotropic scattering when a low-order truncation to a polynomial series solution to equation (5) is used.

Paper II gave the analytic solution of equation (9) for the unscattered particle distribution functions:

$$F(r, t, \mu, v) = F(\tilde{r}_0, 0, \tilde{\mu}_0, \tilde{v}_0)e^{-t/\tau} , \tag{11}$$

with

$$r^2 = \frac{1}{2}\left[\tilde{r}_0^2(1 - \tilde{\mu}_0) + 4U^2(1 + \tilde{\mu}_0)\left(\frac{\tilde{r}_0}{2U} + t\right)^2\right] , \tag{12a}$$

$$v^2 = 2\left(C + U^2 - U\sqrt{U^2 + 2C - \frac{D^2}{r^2}}\right) , \tag{12b}$$

$$\mu = \left(C - \frac{1}{2}v^2\right)\frac{1}{Uv} , \tag{12c}$$

where D and C are constants determined only by the initial condition of the charged particles: $D = \tilde{r}_0 \tilde{v}_0 (1 - \tilde{\mu}_0^2)^{1/2}$ and $C = \frac{1}{2}\tilde{v}_0^2 + \tilde{\mu}_0 U \tilde{v}_0$, where $\tilde{\mu}_0$ and $\tilde{v}_0$ are the pitch angle and speed of particles at the initial location $\tilde{r}_0$. Since equation (12) is essentially the implication of Liouville's theorem, the inverse relation of initial values as function of r, v, μ, and t is simply changing t to $-t$.

To solve the scattered particle distribution, we first expand f^s in an infinite series of Legendre polynomials in the form of

$$f^s = \sum_{n=0}^{\infty} (2n+1) P_n(\mu) f_n \,, \tag{13}$$

where $f_n = 2\pi \int_{-1}^{1} P_n(\mu) f^s(r, t, \mu, v) d\mu$ is the nth harmonic of the distribution functions f^s, and P_n represents the nth Legendre polynomial.

By means of the recursion relations $(n+1)P_{n+1} + nP_{n-1} = (2n+1)\mu P_n$, $\mu P_n' - P_{n-1}' = nP_n$, and $(\mu^2 - 1)P_n' = n\mu P_n - nP_{n-1}$ (the prime denotes differentiation), we obtain an infinite set of partial differential equations for the harmonics of the distribution functions f_n,

$$\begin{aligned} \frac{\partial f_n}{\partial t} + U \frac{\partial f_n}{\partial r} + \frac{(n+1)v}{2n+1} \frac{\partial f_{n+1}}{\partial r} + \frac{nv}{2n+1} \frac{\partial f_{n-1}}{\partial r} + \frac{(n+1)(n+2)}{(2n+1)(2n+3)} \frac{Uv}{r} \frac{\partial f_{n+2}}{\partial v} - \left[1 - \frac{(n+1)^2}{(2n+1)(2n+3)} - \frac{n^2}{(2n-1)(2n+1)}\right] \\ \times \frac{Uv}{r} \frac{\partial f_n}{\partial v} + \frac{n(n-1)}{(2n-1)(2n+1)} \frac{Uv}{r} \frac{\partial f_{n-2}}{\partial v} = \frac{F_n}{\tau} - (n+1)n \frac{f_n}{\tau} - \frac{(n+1)(n+2)}{2n+1} \frac{v}{r} f_{n+1} + \frac{n(n-1)}{2n+1} \frac{v}{r} f_{n-1} \\ - \frac{(n+1)(n+2)(n+3)}{(2n+1)(2n+3)} \frac{U}{r} f_{n+2} - \frac{n(n+1)}{(2n-1)(2n+3)} \frac{U}{r} f_n + \frac{n(n-1)(n-2)}{(2n-1)(2n+1)} \frac{U}{r} f_{n-2} \,, \end{aligned} \tag{14}$$

where the source term F_n is the nth harmonic of the decaying unscattered distribution F, i.e., $F = \sum_{n=0}^{\infty} (2n+1) P_n(\mu) F_n$ and $F_n = 2\pi \int_{-1}^{1} P_n(\mu) F(r, t, \mu, v) d\mu$.

Papers I and II have shown that low-order expansions can be used to investigate particle transport at arbitrarily small times. For the f_1 truncation, equation (14) yields the coupled system

$$\frac{\partial f_0}{\partial t} + U \frac{\partial f_0}{\partial r} + v \frac{\partial f_1}{\partial r} - \frac{2Uv}{3r} \frac{\partial f_0}{\partial v} = \frac{F_0}{\tau} - \frac{2v}{r} f_1 \tag{15}$$

$$\frac{\partial f_1}{\partial t} + U \frac{\partial f_1}{\partial r} + \frac{v}{3} \frac{\partial f_0}{\partial r} - \frac{2Uv}{5r} \frac{\partial f_1}{\partial v} = \frac{F_1}{\tau} - \frac{2f_1}{\tau} - \frac{2U}{5r} f_1 \,. \tag{16}$$

Equations (15) and (16) are very similar to those of Papers I or II, and therefore can be solved numerically by using the operator split procedure described in Papers I and II, together with the analytic solution in the form of equation (11).

3. ANISOTROPIC SMALL-ANGLE SCATTERING AND MQLT MODEL

In space and astrophysical plasma, significant anisotropies are usually observed in the particle distributions. One such example is interstellar pickup ions. At high latitudes or very close to the Sun, where the $\boldsymbol{B}$ field is oriented more radially, the velocity distribution of pickup ions is found to be highly anisotropic, with little scattering into the $V/U > 1$ phase-space hemisphere (Gloeckler et al. 1995; Gloeckler & Geiss 1998). Another example is solar particle events (Palmer 1982). For fully developed MHD turbulence, Kolmogorov theory yields a power spectrum in magnetic fluctuation with an exponent of $-5/3$. In the solar wind, the power spectrum of magnetic fluctuations is frequently a broken power law with an inertial range exponent of $-5/3$ (Matthaeus et al. 1994). To illustrate our approach, we extend the propagating source method to investigate particle transport in such a turbulent medium (i.e., $q = 5/3$).

The nonisotropic diffusion coefficient $D_{\mu\mu}$ in equation (4) is zero at 90°. Particles of large pitch angle experience very slow scattering across 90° when $1 < q < 2$ or are unable to scatter through $\mu = 0$ when $q \geq 2$. Here we do not discuss mechanisms for solving this problem, but simply assume that mirroring is responsible. A combination of mirroring and quasi-linear wave interactions act over all pitch angles, but the quasi-linear interaction dominates in the backward and forward hemisphere, while only the mirror-linear interaction acts to scatter particles at $\theta = 90°$. This assumption is in basic agreement with the recent analysis of Felice & Kulsrud (2001).

In our mathematical model, we introduce a two-timescale, anisotropic scattering operator. In the $\mu < 0$ hemisphere and the $\mu > 0$ hemisphere, the quasi-linear scattering proceeds at the effective rate τ_1^{-1}. However, scattering from one hemisphere to the other in velocity space is due to mirroring, and this effect can be approximated by a BGK relaxation-time operator at an average mirror scattering rate τ_2. As in Paper II, We use f^+ to represent the forward-moving particles ($\mu > 0$), and f^- the backward-moving particles ($\mu < 0$). We have

$$\frac{\partial f^{\mp}}{\partial t} + (U + v\mu)\frac{\partial f^{\mp}}{\partial r} - (1-\mu^2)\frac{Uv}{r}\frac{\partial f^{\mp}}{\partial v} + \frac{1-\mu^2}{r}(v+\mu U)\frac{\partial f^{\mp}}{\partial \mu} = \frac{\partial}{\partial \mu}\left[\frac{\mu^{2/3}(1-\mu^2)}{\tau_1}\frac{\partial f^{\mp}}{\partial \mu}\right] + \frac{\langle f^{\mp}\rangle - f^{\pm}}{\tau_2}\ , \tag{17}$$

where $\langle f^-\rangle = \frac{1}{2}\int_{-1}^{0} f^- d\mu$, $\langle f^+\rangle = \frac{1}{2}\int_0^1 f^+ d\mu$. Obviously, $\tau_2 \gg \tau_1$ means highly anisotropic pitch-angle scattering, i.e., particles are typically scattered many times before being scattered through $\mu = 0$. The above model is denoted the MQLT model to distinguish it from the standard QLT model.

Following the procedure in § 2, we split the distribution function $f^{\mp}$ into scattered and unscattered particle distributions, i.e.,

$$f^{\mp} = F^{\mp}(r, t, \mu, v) + f^{s\mp}(r, t, \mu, v)\ . \tag{18}$$

Then rearranging equation (17) yields

$$\frac{\partial F^{\mp}}{\partial t} + (U + v\mu)\frac{\partial F^{\mp}}{\partial r} - (1-\mu^2)\frac{Uv}{r}\frac{\partial F^{\mp}}{\partial v} + \frac{1-\mu^2}{r}(v+\mu U)\frac{\partial F^{\mp}}{\partial \mu} = -\frac{F^{\mp}}{\bar{\tau}}\ , \tag{19}$$

$$\frac{\partial f^{s\mp}}{\partial t} + (U + v\mu)\frac{\partial f^{s\mp}}{\partial r} - (1-\mu^2)\frac{Uv}{r}\frac{\partial f^{s\mp}}{\partial v} + \frac{1-\mu^2}{r}(v+\mu U)\frac{\partial f^{s\mp}}{\partial \mu} = \frac{\partial}{\partial \mu}\left(\frac{\mu^{2/3}(1-\mu^2)}{\tau_1}\frac{\partial f^{S\mp}}{\partial \mu}\right) + \frac{F^{\mp}}{\tau_1} + \frac{F_0^{\pm}}{\tau_2} + \frac{f_0^{\pm} - f^{s\mp}}{\tau_2}\ , \tag{20}$$

where $F_0^- = \int_{-1}^0 F^-(r,t,\mu,v)d\mu$, $F_0^+ = \int_0^1 F^+(r,t,\mu,v)d\mu$, $f_0^- = \int_{-1}^0 f^{s-}(r,t,\mu,v)d\mu$, and $f_0^+ = \int_0^1 f^{s+}(r,t,\mu,v)d\mu$. Here $\bar{\tau} = \tau_1\tau_2/(\tau_1+\tau_2)$ is the average time of all effective scattering.

The analytic solution of equation (19) for the unscattered particle distributions is

$$F^{\mp}(r, t, \mu, v) = F^{\mp}(\tilde{r}_0, 0, \tilde{\mu}_0, \tilde{v}_0)e^{-t/\bar{\tau}}\ , \tag{21}$$

where r, μ, and v satisfy the equations (12a)–(12c).

To solve (20), we again expand $f^{s\mp}$ in terms of Legendre polynomials,

$$f^{s\mp}(r, t, \mu, v) = \sum_{n=0}^{\infty}(2n+1)P_n(2\mu \pm 1)f_n^{\mp}(r, t, v)\ , \tag{22}$$

where $f_n^+ = \int_0^1 P_n(2\mu - 1)f^{s+}(r,t,\mu,v)d\mu$ and $f_n^- = \int_{-1}^0 P_n(2\mu+1)f^{s-}(r,t,\mu,v)d\mu$ are the nth harmonics of the distribution functions f^{s+} and f^{s-}, respectively. On substituting the Legendre polynomial expansion of equation (22) into equation (20), we obtain an infinite number of partial differential equations in the forward and backward harmonics $f_n^{\mp}$:

$$\begin{aligned}
&\frac{\partial f_n^{\mp}}{\partial t} + \left(U \mp \frac{v}{2}\right)\frac{\partial f_n^{\mp}}{\partial r} + \frac{nv}{2(2n+1)}\frac{\partial f_{n-1}^{\mp}}{\partial r} + \frac{(n+1)v}{2(2n+1)}\frac{\partial f_{n+1}^{\mp}}{\partial r} \mp \frac{n+1}{2(2n+1)}\frac{Uv}{r}\frac{\partial f_{n+1}^{\mp}}{\partial v} + \frac{(n+1)(n+2)}{4(2n+1)(2n+3)}\frac{Uv}{r}\frac{\partial f_{n+2}^{\mp}}{\partial v}\\
&\quad - \left[3(2n+1) - \frac{(n+1)^2}{2n+3} - \frac{n^2}{2n-1}\right]\frac{1}{4(2n+1)}\frac{Uv}{r}\frac{\partial f_n^{\mp}}{\partial v} \mp \frac{n}{2(2n+1)}\frac{Uv}{r}\frac{\partial f_{n-1}^{\mp}}{\partial v} + \frac{(n-1)n}{4(2n-1)(2n+1)}\frac{Uv}{r}\frac{\partial f_{n-2}^{\mp}}{\partial v}\\
&\quad = \delta_{n0}\frac{f_0^{\pm} + F_0^{\pm}}{\tau_2} + \frac{F_n^{\mp}}{\tau_1} - \frac{f_n^{\mp}}{\tau_2} - \frac{(n+1)(n+2)(n+3)}{4(2n+1)(2n+3)}\frac{U}{r}f_{n+2}^{\mp} - \left[\frac{n(n+1)}{4(2n-1)(2n+3)}U \mp (n+1)v\right]\frac{1}{r}f_n^{\mp}\\
&\qquad - \frac{(n+1)(n+2)}{2(2n+1)}\frac{v \mp 3U/2}{r}f_{n+1}^{\mp} + \frac{(n-1)n}{2(2n+1)}\frac{v \mp 3U/2}{r}f_{n-1}^{\mp} + \frac{(n-2)(n-1)n}{4(2n-1)(2n+1)}\frac{U}{r}f_{n-2}^{\mp} + Q_1 - Q_2\ ,
\end{aligned} \tag{23}$$

where the source term $F_n^{\mp}$ is the nth harmonic of the decaying unscattered distribution $F^{\mp}$, i.e., $F_n^+ = \int_0^1 P_n(2\mu - 1)$ $F^+(r,t,\mu,v)d\mu$ and $F_n^- = \int_{-1}^0 P_n(2\mu+1) \times F^-(r,t,\mu,v)d\mu$. Here Q_1 and Q_2 are given by

$$\begin{aligned}
Q_1 = \frac{n}{\sqrt[3]{4}\tau_1}\Bigg\{ &-3(n+1)f_n^{\mp} - \frac{n+3}{3(2n+1)} \times \left[\frac{(n+1)(n+2)f_{n+2}^{\mp} + (n+1)^2 f_n^{\mp}}{2n+3} + \frac{n^2 f_n^{\mp} + n(n-1)f_{n-2}^{\mp}}{2n-1}\right]\\
&\pm \frac{2(n+1)(n+4)}{9(2n+1)(2n+3)}\left[(n+2)\frac{(n+3)f_{n+3}^{\mp} + (n+2)f_{n+1}^{\mp}}{2n+5} + (n+1)\frac{(n+1)f_{n+1}^{\mp} + nf_{n-1}^{\mp}}{2n+1}\right]\\
&\pm \frac{2n(n+4)}{9(2n+1)(2n-1)}\left[\frac{n(n+1)f_{n+1}^{\mp} + n^2 f_{n-1}^{\mp}}{2n+1} + (n-1)\frac{(n-1)f_{n-1}^{\mp} + (n-2)f_{n-3}^{\mp}}{2n-3}\right]\\
&+ \frac{2}{3}\frac{nf_n^{\mp} + (n-1)f_{n-2}^{\mp}}{(2n-1)} \mp \frac{2}{3}\frac{1}{2n-1}\left[\frac{n(n+1)f_{n+1}^{\mp} + n^2 f_{n-1}^{\mp}}{2n+1} + \frac{(n-1)^2 f_{n-1}^{\mp} + (n-2)(n-1)f_{n-3}^{\mp}}{2n-3}\right]\Bigg\}\ ,
\end{aligned} \tag{24}$$

and

$$Q_2 = (\pm 1)^{n+1}\frac{v}{2r}f^{\mp}(\mu=0) - \begin{cases} \dfrac{n}{4}\dfrac{v}{r}\displaystyle\int_{-1}^{0}\dfrac{1}{\mu}(P_n(2\mu+1) - P_{n-1}(2\mu+1))f^{-}d\mu & \text{for } f_n^- , \\ \dfrac{n}{4}\dfrac{v}{r}\displaystyle\int_{0}^{1}\dfrac{1}{\mu}(P_n(2\mu-1) + P_{n-1}(2\mu-1))f^{+}d\mu & \text{for } f_n^+ . \end{cases} \tag{25}$$

For the $f_1^{s\mp}$ approximation, we have $f^{s\mp} = P_0 f_0^{\mp} + 3P_1 f_1^{\mp} = f_0^{\mp} + 3(2\mu \pm 1)f_1^{\mp}$. Thus, equations (23) reduce to

$$\frac{\partial f_0^{\mp}}{\partial t} + \left(U \mp \frac{v}{2}\right)\frac{\partial f_0^{\mp}}{\partial r} + \frac{v}{2}\frac{\partial f_1^{\mp}}{\partial r} - \frac{2Uv}{3r}\frac{\partial f_0^{\mp}}{\partial v} \mp \frac{Uv}{2r}\frac{\partial f_1^{\mp}}{\partial v} = \frac{F_0^{\mp}}{\tau_1} - \frac{f_0^{\mp}}{\tau_2} + \frac{f_0^{\pm} + F_0^{\pm}}{\tau_2} \pm \frac{v}{2r}f_0^{\mp} - \frac{5v \mp 3U}{2r}f_1^{\mp} , \tag{26}$$

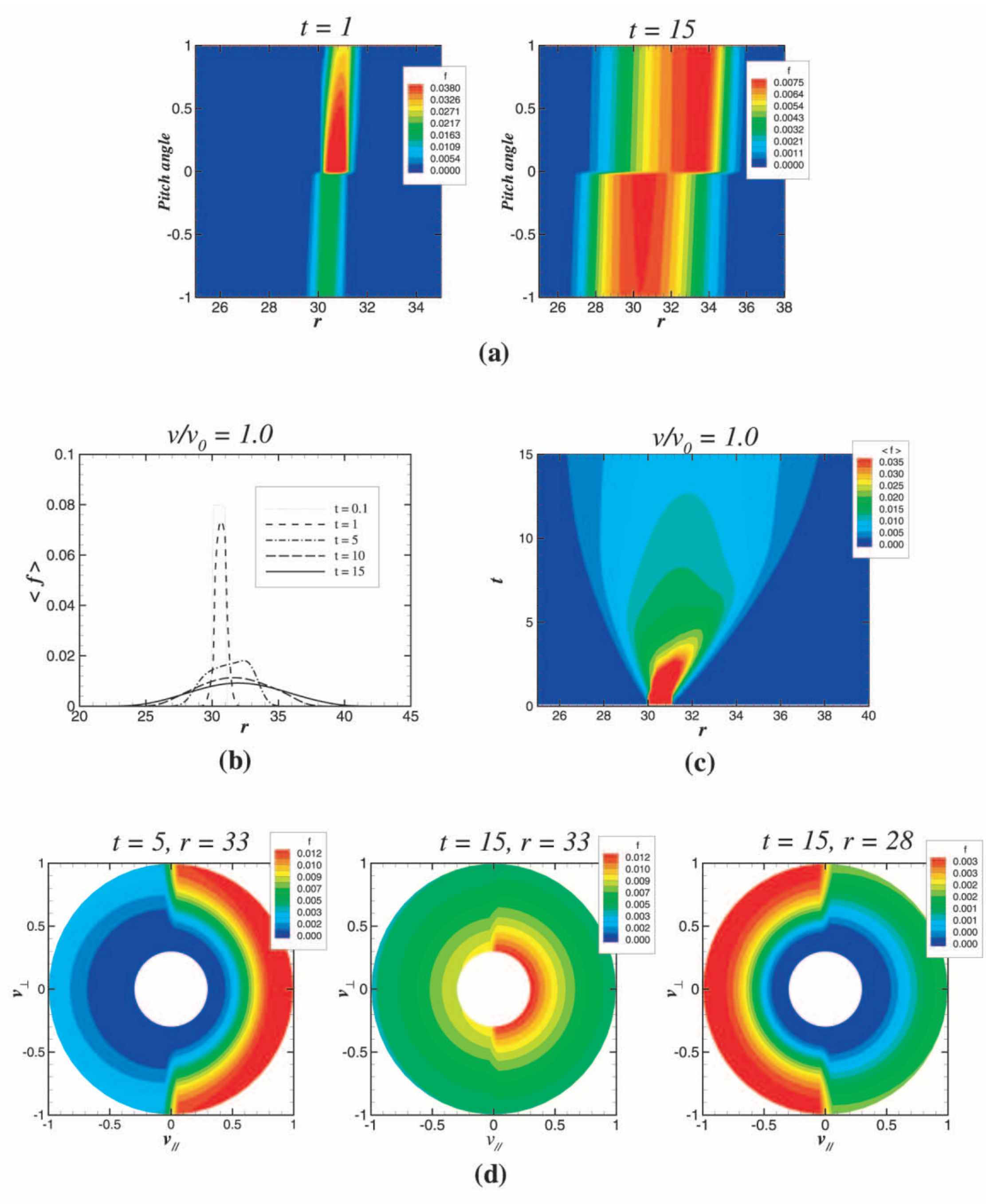

FIG. 1.—MQLT solution of a ring beam for fast particles, $v_0/U = 10$, in a moderately anisotropic scattering $\tau_2/\tau_1 = 3$. (*a*) Distribution function f in pitch angle μ and position r at $t = 1$ and 15. (*b*) Spatial distribution of the omnidirectional distribution $\langle f \rangle$ at $v/v_0 = 1$ when $t = 0.1$, 1, 5, 10, and 15. (*c*) Spatial and temporal evolution of $\langle f \rangle$ at $v/v_0 = 1$. (*d*) Particle distribution in velocity phase space at $r = 3$ when $t = 5$ and 15, and at $r = 28$ when $t = 15$.

$$\frac{\partial f_1^{\mp}}{\partial t} + \left(U \mp \frac{v}{2}\right)\frac{\partial f_1^{\mp}}{\partial r} + \frac{v}{6}\frac{\partial f_0^{\mp}}{\partial r} - \frac{3Uv}{5r}\frac{\partial f_1^{\mp}}{\partial v} \mp \frac{Uv}{6r}\frac{\partial f_0^{\mp}}{\partial v} = \frac{F_1^{\mp}}{\tau_1} - \frac{f_1^{\mp}}{\tau_2} - \frac{46\sqrt[3]{2}}{15}\frac{f_1^{\mp}}{\tau_1} + \frac{1}{2}\frac{v}{r}(f_0^{\mp} \pm f_1^{\mp}) - \frac{1}{10}\frac{U}{r}f_1^{\mp} . \tag{27}$$

Equations (26) and (27) are of the same form as given in Paper II (eq. [29]), with the only difference residing in the right-hand source terms. Therefore, the operator-splitting approach of Paper II can be used directly.

4. COMPARISON OF BGK AND MQLT

It was shown in Paper III that the QLT isotropic and anisotropic models could be rather well approximated by relaxation time scattering models for the Boltzmann equation in the absence of focusing and adiabatic deceleration. We consider here whether this conclusion continues to hold when focusing and adiabatic deceleration are included.

Consider an initial ring beam distribution

$$F^{+}(\tilde{r}_0, t = 0, \tilde{\mu}_0, \tilde{v}_0) = \frac{N(\tilde{r}_0)\delta(\tilde{v}_0 - v_0)\delta(\tilde{\mu}_0 - \mu_0)}{2\pi\tilde{v}_0^2} . \tag{28}$$

In our calculation, the initial beam is located at the region $30 < \tilde{r}_0 < 31$, and $\mu_0 = 0.25$. For the unscattered particles, from equation (21) and the average over μ we have

$$F_0^{+}(r, t, v) = \frac{N(\tilde{r}_0)\delta(\tilde{v}_0 - v_0)}{4\pi\tilde{v}_0^2} e^{-t/\bar{\tau}} . \tag{29}$$

Two anisotropic scattering rates are considered: $\tau_2/\tau_1 = 3$, corresponding to strong scattering of particles through 90°, and $\tau_2/\tau_1 = 10$, corresponding to weak scattering through 90°. The first represents a nearly isotropic scattering model, but the second model is highly anisotropic.

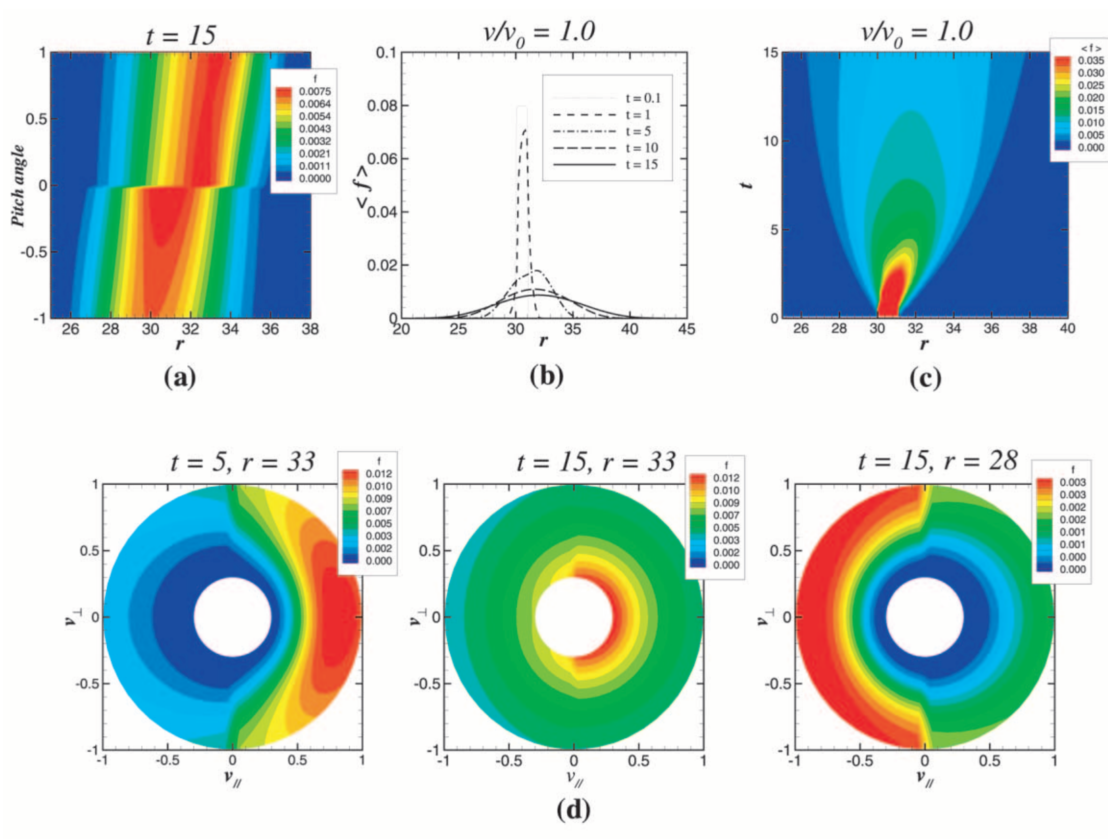

FIG. 2.—BGK solution of a ring beam for fast particles, $v_0/U = 10$, in a moderately anisotropic scattering $\tau_2/\tau_1 = 3$. (*a*) Distribution function f in pitch angle μ and position r at $t = 15$. (*b*) Spatial distribution of the omnidirectional distribution $\langle f \rangle$ at $v/v_0 = 1$ when $t = 0.1$, 1, 5, 10, and 15. (*c*) Spatial and temporal evolution of $\langle f \rangle$ at $v/v_0 = 1$. (*d*) Particle distribution in velocity phase space at $r = 3$ when $t = 5$ and 15, and at $r = 28$ when $t = 15$.

4.1. *Fast Particles:* $v_0/U = 10$

Figure 1 shows solutions of the MQLT model in the presence of strong particle scattering through 90°, $\tau_2/\tau_1 = 3$, for very fast particles, $v_0/U = 10$. Figure 1*a* gives the spatial and pitch-angle distribution for two different normalized times. At early times $t = 1$, the distribution remains highly anisotropic. By $t = 15$, the distribution evolves into an isotropic state in pitch angle and the spatial distribution at a particular pitch angle occupies a region of $\Delta r \sim 8$. Figure 1*b* shows the omnidirectional distribution $\langle f \rangle$ for a particular $v/v_0 = 1.0$. The ring beam at $t = 0.1$ dominates initially before finally evolving into a broad Gaussian distribution by $t = 10$. A related color plot is given in Figure 1*c*, which shows the temporal evolution and spatial distribution of $\langle f \rangle$ at $v/v_0 = 1$. Figure 1*d* shows a two-dimensional color intensity plot in velocity phase space. Here $v_\parallel$ and $v_\perp$ denote the velocities parallel and perpendicular to the magnetic field, respectively. At $t = 5$, $r = 33$, the forward-moving particles have not experienced strong adiabatic cooling. However, by $t = 15$, the right hemisphere exhibits a very strong cooling and the distribution is isotropic within each hemisphere. At $t = 15$, $r = 28$, the backward-moving particles dominate but have not experienced very much cooling. Note that the blank areas in the velocity distribution are not physical limits for the deceleration at the given time, but due to the numerical boundary we used in our calculations.

Figure 2 shows solutions from the relaxation time scattering (BGK) model in Paper II for the same model parameters as in Figure 1. Compared with the MQLT results of Figure 1, the backward-moving particles now take longer to evolve into an isotropic state (Fig. 2*a*), and the anisotropy in velocity phase space persists for a little longer (see $t = 5$, $r = 33$ in Fig. 2*d*). However, there are no significant differences between these two sets of results.

Figure 3 shows solutions from the MQLT model for weak scattering of particles through 90°, $\tau_2/\tau_1 = 10$. As before, the distribution at $t = 15$ is isotropic within each hemisphere (Fig. 3*a*). However, the spatial distribution at a particular pitch angle is now much broader, with $\Delta r \sim 16$ (Fig. 3*a*). The ring beam still dominates at $t = 0.1$. Since particles have difficulty being scattered through 90°, a rightward-moving pulse with a spatially extended flat tail is formed, and the forward-moving particles dominate (Fig 3*b*). A related color plot is also given in Figure 3*c*, which shows the temporal evolution and spatial distribution of $\langle f \rangle$ at $v/v_0 = 1$. In the two-dimensional color intensity plot in velocity phase space shown in Figure 3*d*, the forward-moving particles have not experienced important adiabatic cooling at $t = 5$ and $r = 33$. At $t = 15$, both the forward and backward hemisphere exhibit very strong cooling, and the distribution is isotropic everywhere. At $t = 15$, $r = 28$, the backward-moving particles also experienced important cooling. A comparison of the moderately and the highly anisotropic scattering MQLT

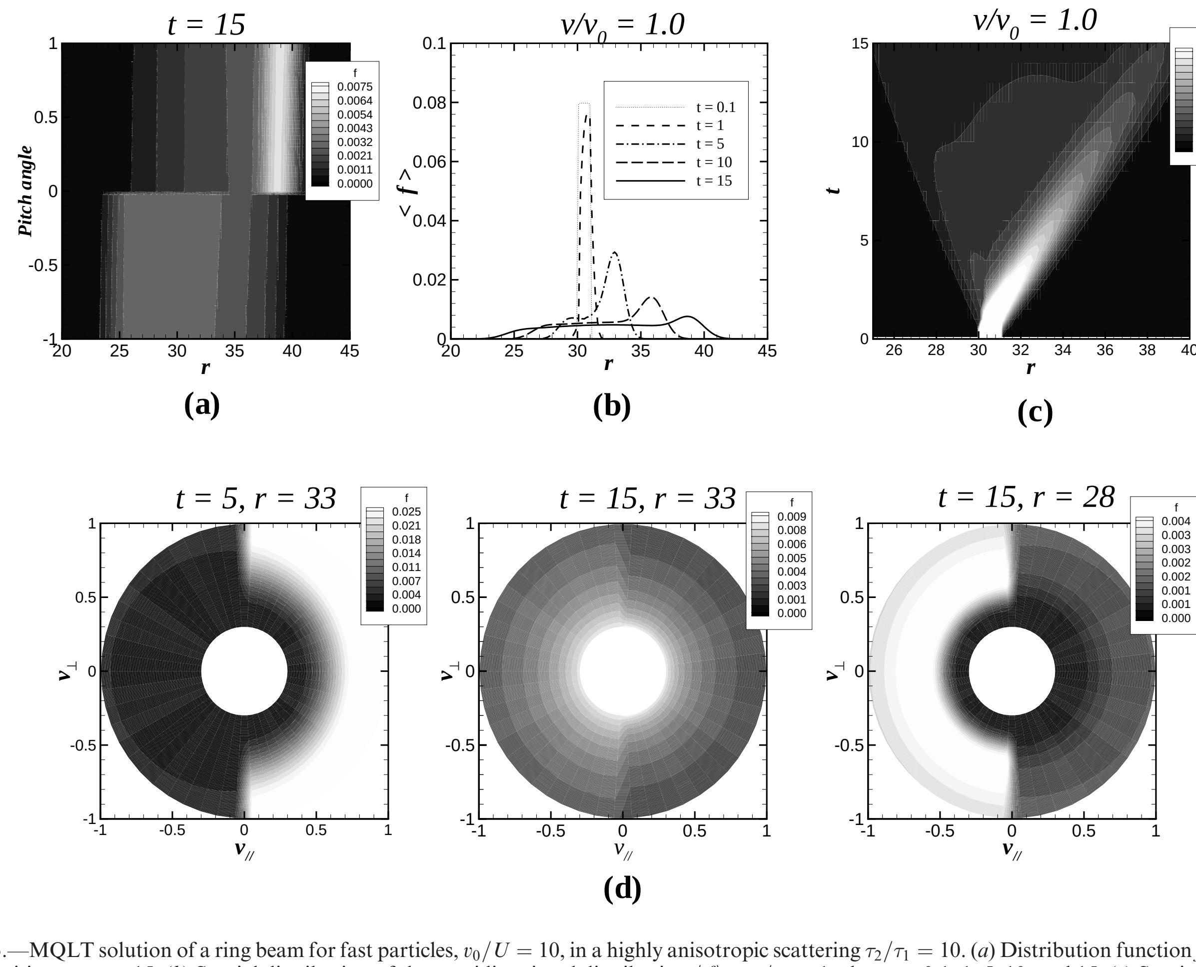

FIG. 3.—MQLT solution of a ring beam for fast particles, $v_0/U = 10$, in a highly anisotropic scattering $\tau_2/\tau_1 = 10$. (*a*) Distribution function *f* in pitch angle μ and position r at $t = 15$. (*b*) Spatial distribution of the omnidirectional distribution $\langle f \rangle$ at $v/v_0 = 1$ when $t = 0.1$, 1, 5, 10, and 15. (*c*) Spatial and temporal evolution of $\langle f \rangle$ at $v/v_0 = 1$. (*d*) Particle distribution in velocity phase space at $r = 3$ when $t = 5$ and 15, and at $r = 28$ when $t = 15$. [*See the electronic edition of the Journal for a color version of this figure.*]

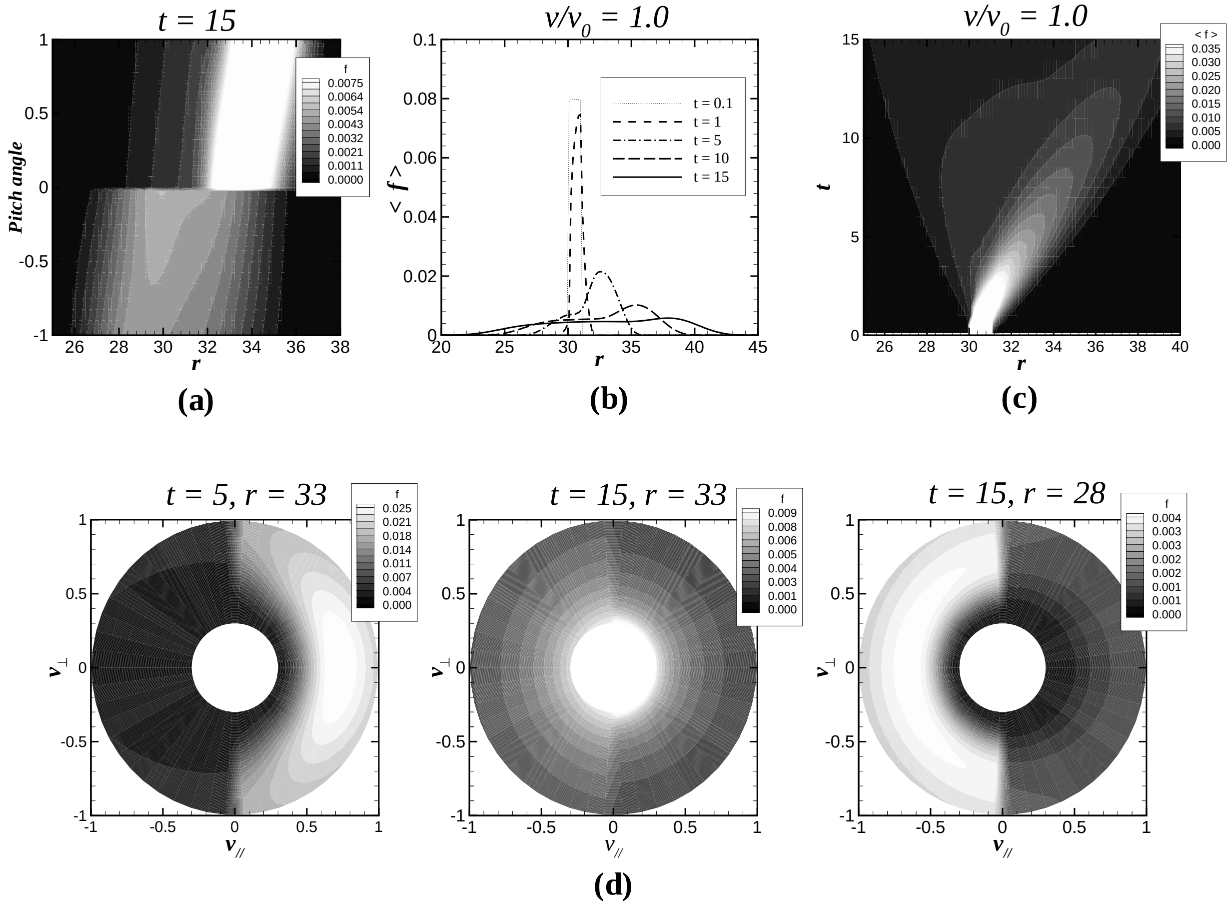

FIG. 4.—BGK solution of a ring beam for fast particles, $v_0/U = 10$, in a highly anisotropic scattering $\tau_2/\tau_1 = 10$. (*a*) Distribution function *f* in pitch angle μ and position *r* at $t = 15$. (*b*) Spatial distribution of the omnidirectional distribution $\langle f \rangle$ at $v/v_0 = 1$ when $t = 0.1$, 1, 5, 10, and 15. (*c*) Spatial and temporal evolution of $\langle f \rangle$ at $v/v_0 = 1$. (*d*) Particle distribution in velocity phase space at $r = 3$ when $t = 5$ and 15, and at $r = 28$ when $t = 15$. [*See the electronic edition of the Journal for a color version of this figure*.]

models suggests that (1) more particles are cooled by adiabatic deceleration, but some particles move a little faster in the highly anisotropic scattering medium (see Figs. 3*d* and 3*b*), and (2) for the same pitch angle, the spatial distribution is much more dispersed in the case of highly anisotropic scattering (see Fig. 3*a*).

Figure 4 shows the solutions of the BGK model in Paper II for the same model parameters as in Figure 3. The evolution of the omnidirectional distributions from the BGK and the MQLT models is very similar, except that some particles move a little slower, and intensity profiles have a greater amplitude at later times in the MQLT model (see Fig. 4*b*). The velocity distributions at $r = 33$ when $t = 5$ and $r = 15$ when $t = 15$ still remain anisotropic in the BGK models (Fig. 4*d*). For a particular pitch angle, the spatial distribution occupies a much narrower region ($\Delta r \sim 9$) than that in the MQLT model, and is only a little wider than that of the moderately anisotropic scattering case (see Fig. 4*a*).

4.2. *Slow Particles:* $v_0/U = 1$

Figure 5 shows solutions from a MQLT model in which strong scattering of particles through 90° occurs, $\tau_2/\tau_1 = 3$, but now for slow particles, $v_0/U = 1$. Although convection is now important, the character of the evolving distribution is very similar to that of the fast-particle example shown in Figure 1, i.e., at early times $t = 1$, the distribution remains highly anisotropic, but by $t = 15$, the distribution evolves toward isotropy in pitch angle, and the spatial distribution at a particular pitch angle occupies a region of $\Delta r \sim 10$ (Fig. 5*a*). The convecting ring beam at $t = 0.1$ propagates to the right and left, and evolves into a broad Gaussian distribution at $t = 10$ (Figs. 5*b* and 5*c*). In velocity phase space at $t = 3$ and $r = 36$, the forward-moving particles in the forward hemisphere dominate and experience some adiabatic cooling, and the distribution is close to isotropy. However, at the same location when $t = 7$, the backward-moving particles dominate because of convection and have experienced significant cooling, with the result that the distribution becomes more isotropic. At $t = 7$, $r = 40$, the forward-moving particles dominate, experiencing important adiabatic cooling, and the distribution is also isotropic.

Figure 6 shows solutions from the BGK model of Paper II for the same model parameters as used in Figure 5. Compared with Figure 5, there exist some slight differences in pitch-angle and velocity distributions. At $t = 7$, $r = 36$ and $t = 7$, $r = 40$, the particle distribution in velocity phase space is not as isotropic as the MQLT model (Fig. 6*d*). However, this difference is

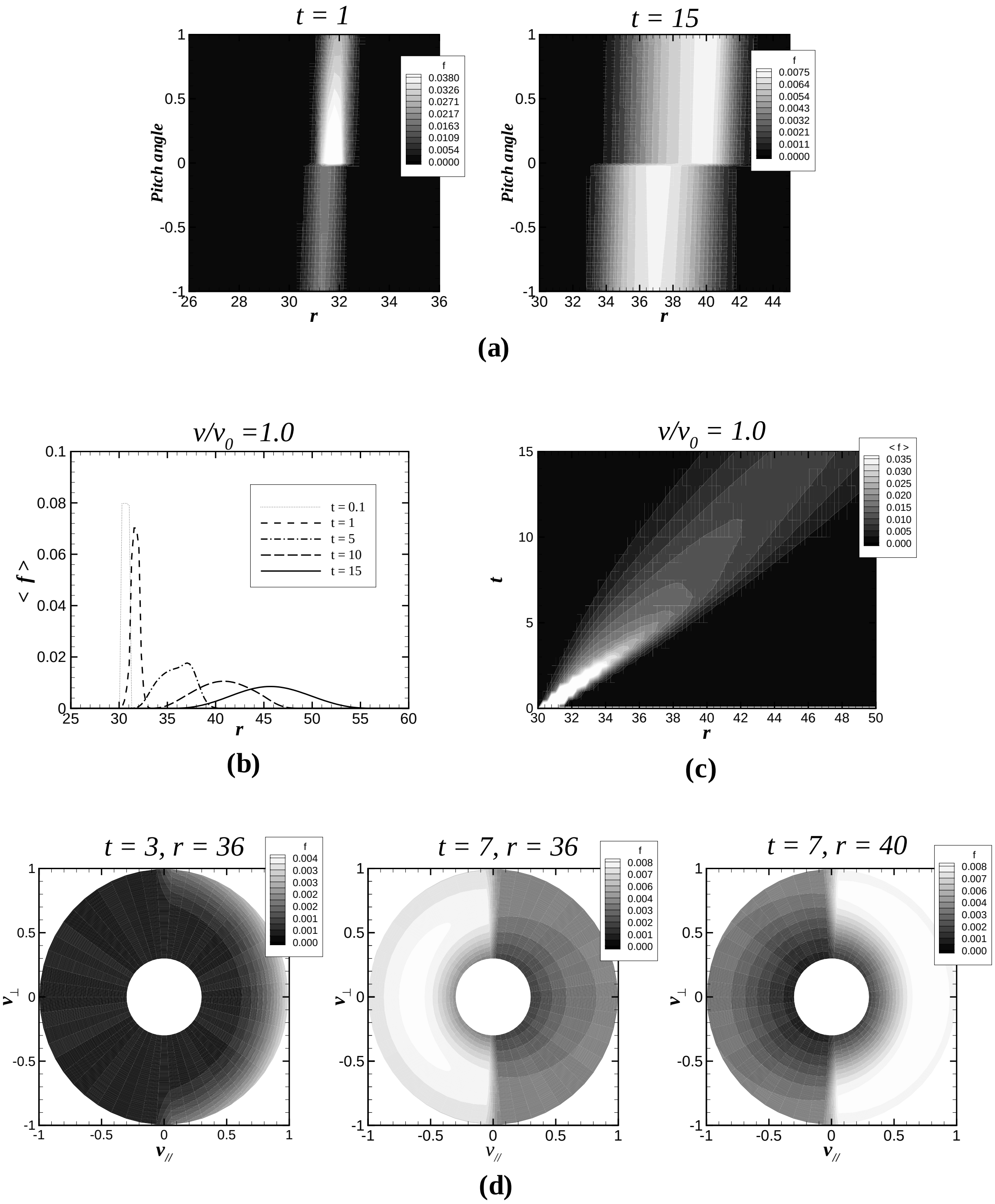

FIG. 5.—MQLT solution of a ring beam for slow particles, $v_0/U = 1$, in a moderately anisotropic scattering $\tau_2/\tau_1 = 3$. (*a*) Distribution function f in pitch angle μ and position r at $t = 1$ and 15. (*b*) Spatial distribution of the omnidirectional distribution $\langle f \rangle$ at $v/v_0 = 1$ when $t = 0.1$, 1, 5, 10, and 15. (*c*) Spatial and temporal evolution of $\langle f \rangle$ at $v/v_0 = 1$. (*d*) Particle distribution in velocity phase space at $r = 36$ when $t = 3$ and 7, and at $r = 40$ when $t = 7$. [*See the electronic edition of the Journal for a color version of this figure*.]

small enough to suggest that the simple relaxation time operator is a reasonable approximation to the MQLT operator for a moderately scattering medium, at least when $q = 5/3$.

Figure 7 shows solutions from a MQLT model with weak scattering of particles through 90°, $\tau_2/\tau_1 = 10$. The evolving distribution in this case is similar to that of the fast particles illustrated in Figure 3 except that convection effects are stronger. At $t = 15$, the distribution is isotropic within each hemisphere, and the spatial distribution at a particular pitch angle occupies a very wide region ($\Delta r \sim 20$; Fig. 7*a*). In the evolution of the omnidirectional distribution $\langle f \rangle$ shown in Figures 7*b* and 7*c*, a rightward-propagating pulse with an extended flat tail is formed, and the forward-moving particles dominate. Figure 7*d* shows a two-dimensional color intensity plot in velocity phase space. At $t = 3$, $r = 36$, the forward-moving particles have experienced some adiabatic cooling. At $t = 7$, forward-moving particles convect away to be replaced by a population of backward-

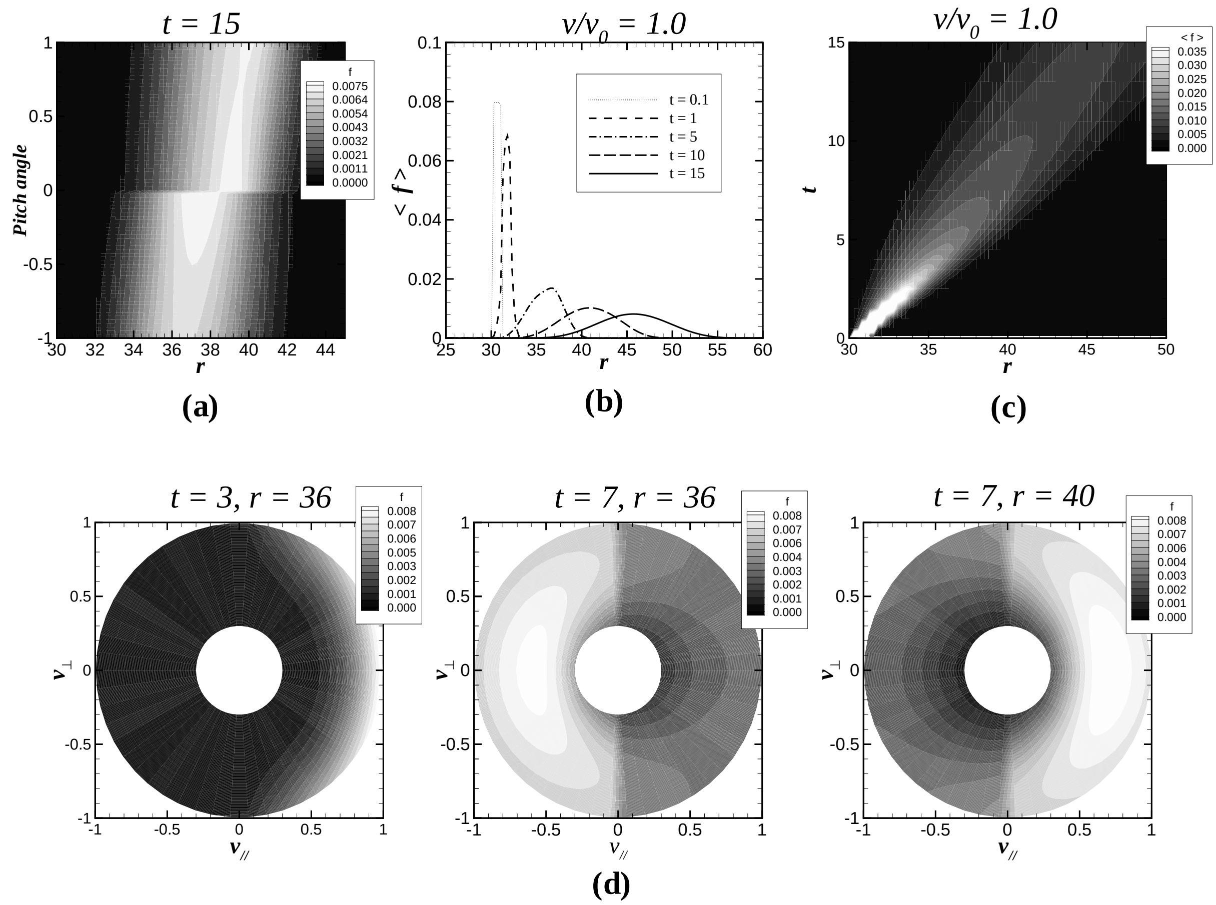

FIG. 6.—BGK solution of a ring beam for slow particles, $v_0/U = 1$, in a moderately anisotropic scattering $\tau_2/\tau_1 = 3$. (*a*) Distribution function f in pitch angle μ and position r at $t = 15$. (*b*) Spatial distribution of the omnidirectional distribution $\langle f \rangle$ at $v/v_0 = 1$ when $t = 0.1$, 1, 5, 10, and 15. (*c*) Spatial and temporal evolution of $\langle f \rangle$ at $v/v_0 = 1$. (*d*) Particle distribution in velocity phase space at $r = 36$ when $t = 3$ and 7, and at $r = 40$ when $t = 7$. [*See the electronic edition of the Journal for a color version of this figure.*]

moving particles, which have cooled and are partially isotropic. At $t = 7$, $r = 40$, the forward-moving particles have experienced significant cooling and the distribution is isotropic. The differences between the moderately and highly anisotropic scattering models for fast particles continues to hold for the slow particles.

Figure 8 shows solutions from the BGK model in Paper II for the same model parameters as in Figure 7. As before, the solution of the distributions governed by the MQLT and BGK models exhibits only small differences.

5. SUMMARY

The propagating source method for solving the Fokker-Planck equation has been extended to a generalized case that includes small- and/or large-angle scattering, focusing, and adiabatic deceleration in a radial magnetic field. Specifically, in this paper we have considered a MQLT model, i.e., a standard QLT pitch-angle scattering within each hemisphere, plus a mirror-linear interaction that is responsible for scattering through 90°. We furthermore compare the results from the QLT isotropic and MQLT anisotropic models with those from relaxation time scattering (BGK) models for an initial ring beam distribution in the cases of fast and slow particles. We present the detailed numerical technique for two specific power spectra, $q = 1$ and 5/3. The first spectrum corresponds to isotropic scattering, and the second is the Kolmogorov spectrum, which is frequently observed in the solar wind fluctuations. However, the technique developed here can be applied to arbitrary spectra.

This paper and our previous papers in this series have developed an effective and accurate numerical approach to solving the Fokker-Planck equation. A comprehensive investigation of various solutions has been presented. We summarize our results as follows:

1. The particle distribution function can be separated into an unscattered part and a scattered part. By using Legendre polynomial expansions, the Boltzmann equation can be reduced to an infinite series of partial differential equations in the harmonics of polynomial expansions.
2. In the absence of focusing and adiabatic deceleration, the lowest order truncation of the coupled set of equations yields an inhomogeneous form of the telegrapher equation. Unlike the homogeneous telegrapher equation, the inhomogeneous telegrapher equation does not introduce physically unrealistic pulse solutions.

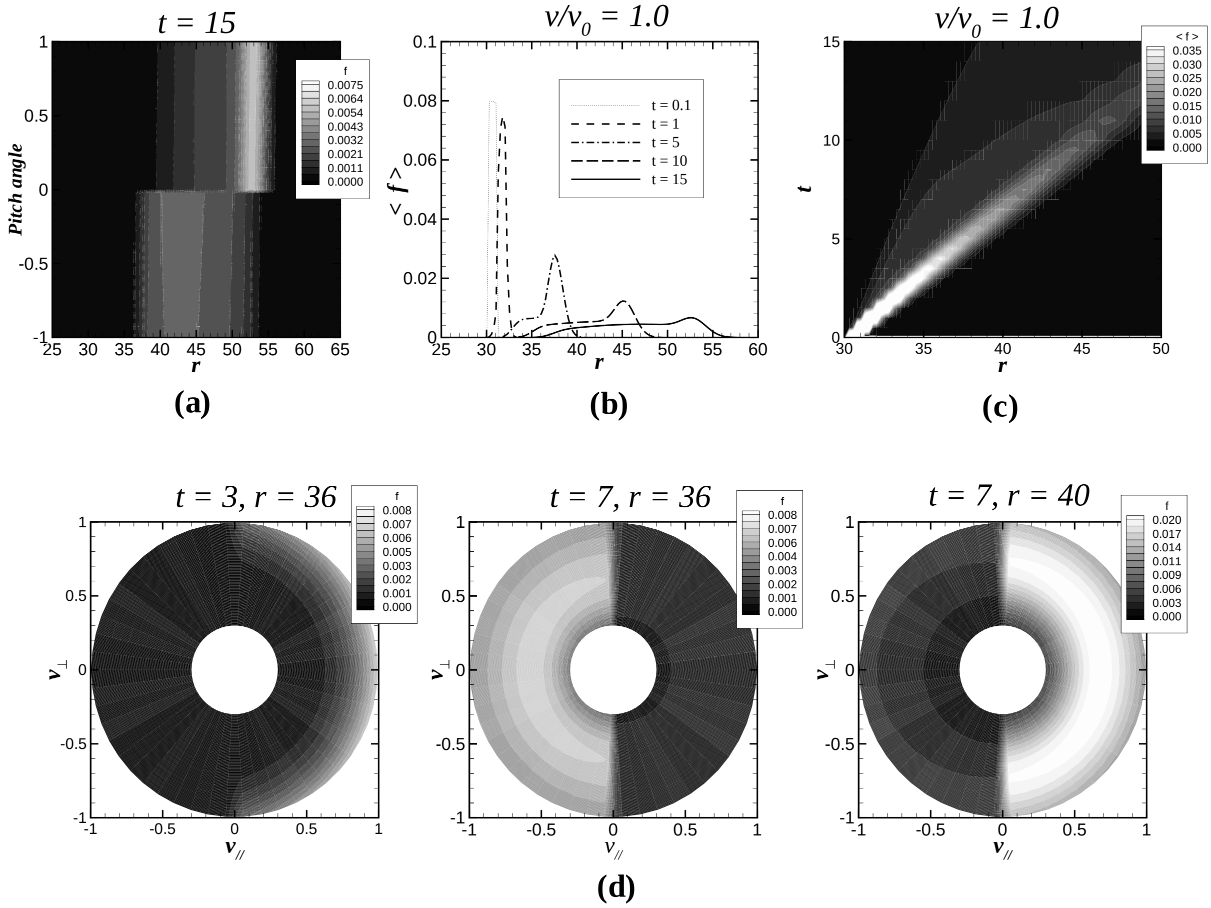

FIG. 7.—MQLT solution of a ring beam for slow particles, $v_0/U = 1$, in a highly anisotropic scattering $\tau_2/\tau_1 = 10$. (*a*) Distribution function f in pitch angle μ and position r at $t = 15$. (*b*) Spatial distribution of the omnidirectional distribution $\langle f \rangle$ at $v/v_0 = 1$ when $t = 0.1$, 1, 5, 10, and 15. (*c*) Spatial and temporal evolution of $\langle f \rangle$ at $v/v_0 = 1$. (*d*) Particle distribution in velocity phase space at $r = 36$ when $t = 3$ and 7, and at $r = 40$ when $t = 7$. [*See the electronic edition of the Journal for a color version of this figure*.]

3. Low-order truncations can be used to investigate particle propagation and transport in an isotropic/anisotropic scattering medium. A powerful and accurate numerical technique, a characteristic method with operator splitting, is developed. A decided advantage of this approach over others is its ability to model nonisotropic initial data easily.
4. For an isotropic or a moderately anisotropic pitch-angle scattering, the initial ring-beam distribution finally evolves into a broad Gaussian distribution, and the QLT isotropic and MQLT anisotropic models could be rather well approximated by the simple relaxation time operator.
5. For a highly anisotropic pitch-angle scattering, a moving pulse with a spatially extended flat tail is formed, and there exist some differences between the MQLT and BGK models. Specifically, at a particular pitch angle, the spatial distribution from MQLT model occupies a much wider region than that in the BGK model.
6. In the highly anisotropic scattering medium, more particles are cooled by adiabatic deceleration, some particles move a little faster, and the spatial distribution at a specific pitch angle is much more dispersed than that in the case of moderately anisotropic scattering.
7. Compared with the BGK model, the anisotropy persists for a little longer and some particles move a little slower; consequently, intensity profiles have a greater amplitude at later times in the MQLT model. For a particular pitch angle, the spatial distribution from the BGK model occupies a much narrower region than the MQLT model.
8. Fast and slow particles have similar distribution characteristics except that convection is much more important for slow particles.

In our work, we have not considered perpendicular diffusion and drifts. As pointed out by Webb et al. (2001), in a nonuniform magnetic field there may exist nonzero contributions to the divergence of the particle current due to curvature and gradient drifts associated with the antisymmetric diffusion coefficient. Further work that incorporates the effects of drifts and cross-field diffusion in an arbitrary magnetic field topology is required.

J. Y. L. benefited from Y. C. Whang in the programming. J. Y. L., R. R., and R. M. are supported by the Canadian Space Agency, the Natural Science and Engineering Research Council of Canada. G. P. Z. is supported in part by NASA grants NAG5-10932 and NAGS-11393, and NSF grants ATM-0296113 and ATM-0296114.

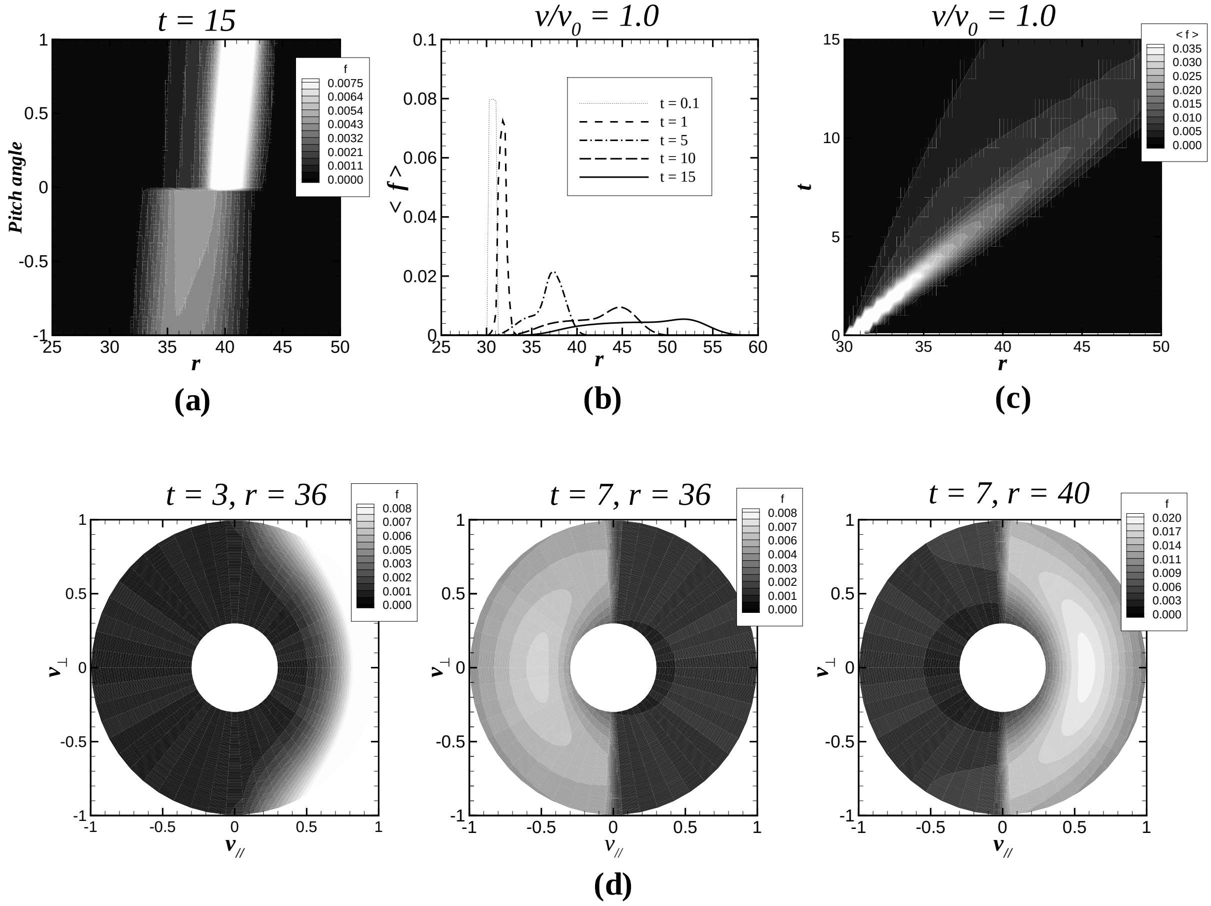

FIG. 8.—BGK solution of a ring beam for slow particles, $v_0/U = 1$, in a highly anisotropic scattering $\tau_2/\tau_1 = 10$. (*a*) Distribution function *f* in pitch angle μ and position *r* at $t = 15$. (*b*) Spatial distribution of the omnidirectional distribution $\langle f \rangle$ at $v/v_0 = 1$ when $t = 0.1$, 1, 5, 10, and 15. (*c*) Spatial and temporal evolution of $\langle f \rangle$ at $v/v_0 = 1$. (*d*) Particle distribution in velocity phase space at $r = 36$ when $t = 3$ and 7, and at $r = 40$ when $t = 7$. [*See the electronic edition of the Journal for a color version of this figure.*]

REFERENCES

Bieber, J. W., & Matthaeus, W. H. 1991, Proc. 22d Int. Cosmic-Ray Conf. (Dublin), 3, 248
———. 1992, in AIP Conf. Proc. 264, Particle Acceleration in Cosmic Plasmas, ed. G. P. Zank & T. K. Gaisser (New York: AIP), 86
Bieber, J. W., Matthaeus, W. H., Smith, C. W., Wanner, W., Kallenrode, M.-B., & Wibberenz, G. 1994, ApJ, 420, 294
Dröge, W. 2000a, ApJ, 537, 1073
———. 2000b, Space Sci. Rev., 93, 121
Dröge, W., & Schlickeiser, R. 1993, Proc. 23d Int. Cosmic-Ray Conf. (Calgary), 3, 199
Fedorov, Yu. I., Stehlik, M., & Kudela K. 1999, Proc. 26th Int. Cosmic-Ray Conf. (Salt Lake City), 6, 348
Felice, G. M., & Kulsrud, R. M. 2001, ApJ, 553, 198
Fisk, L. A., & Axford, W. I. 1969, Sol. Phys., 7, 46
Gloeckler, G., & Geiss J. 1998, Space Sci. Rev., 86, 127
Gloeckler, G., Schwadron, N. A., Fisk, L. A., & Geiss, J. 1995, Geophys. Res. Lett., 22, 2665
Goldstein, M. L. 1976, ApJ, 204, 900
Goldstein, M. L., Klimas, A. J., & Sandri, G. 1975, ApJ, 195, 787
Gombosi, T. I., Jokipii, J. R., Kóta, J., Lorencz, K., & Williams, L. L. 1993, ApJ, 403, 377
Gombosi, T. I., Neugebauer, M., Johnstone, A. D., Coates, A. J., & Huddleston, D. E. 1991, J. Geophys. Res., 96, 9467
Hasselmann, K., & Wibberenz, G. 1968, Z. Geophys., 34, 353
Isenberg, P. A. 1997, J. Geophys. Res., 102, 4719
Jokipii, J. R. 1966, ApJ, 146, 480
Jones, F. C., Birmingham, T. J., & Kaiser, T. B. 1978, Phys. Fluids, 21, 347
Kóta, J. 1994, ApJ, 427, 1035
Kulsrud, R. M. 1983, in Basic Plasma Physics, Vol. I, ed. A. A. Galeev & R. N. Sudan (New York: North-Holland), 115
Lu, J. Y., & Zank, G. P. 2001, J. Geophys. Res., 106, 5709
Lu, J. Y., Zank, G. P., & Webb, G. M. 2001, ApJ, 550, 34 (Paper II)
Matthaeus, W. H., Oughton, S., Pontius, D., & Zhou Y. 1994, J. Geophys. Res., 99, 19267
Owens, A. J. 1974, ApJ, 191, 235
Palmer, I. D. 1982, Rev. Geophys. Space Phys., 20, 335
Ragot, B. R. 1999, ApJ, 518, 974
———. 2000, ApJ, 536, 455
Schlickeiser, R. 1988, J. Geophys. Res., 93, 2725
———. 1989, ApJ, 336, 243
Schlickeiser, R., Dung, R., & Haekel, U. 1991, A&A, 242, L5
Schwadron, N. A. 1998, J. Geophys. Res., 103, 20643
Skilling, J. 1971, ApJ, 170, 265
Smith, C. W. 1992, in AIP Conf. Proc. 264, Particle Acceleration in Cosmic Plasmas, ed. G. Zank & T. Gaisser (New York: AIP), 79
Völk, H. J. 1973, Ap&SS, 25, 471
———. 1975, Rev. Geophys. Space Phys., 13, 547
Webb, G. M., Kota, J., Zank, G. P., & Lu, J. Y. 2001, Proc. 27th Int. Cosmic-Ray Conf. (Hamburg), 8, 3326
Webb, G. M., Pantazopoulou, M., & Zank, G. P. 2000, J. Phys. A, 33, 3137
Webb, G. M., Zank, G. P., Pantazopoulou, M., & Zakharian, A. K. 1999, Proc. 26th Int. Cosmic-Ray Conf. (Salt Lake City), 6, 351
Zank, G. P., Lu, J. Y., & Dröge W. 2002, J. Plasma Phys., in press (Paper III)
Zank, G. P., Lu, J. Y., Rice, W. K. M., & Webb, G. M. 1999, Proc. 26th Int. Cosmic-Ray Conf. (Salt Lake City), 6, 312
———. 2000, J. Plasma Phys., 64, 507 (Paper I)